Journal of the Korean Nuclear Society
Volume 14, Number 4 December, 1982

≪Original≫

A Finite Element Solution to the Group Diffusion Problems with Albedo-Type Boundary Conditions

Kun Joong Yoo
Korea Advanced Energy Research Institute
Chang Hyo Kim · Chang Hyun Chung
Seoul National University

(Received September 13, 1982)

Albedo형 경계조건을 가진 다군확산문제에 대한 유한요소해

유 건 중
한국에너지연구소
김 창 효 · 정 창 현
서울대학교

(1982. 9. 13 접수)

Abstract

Albedo-type boundary condition is incorporated into the finite element formulation of the cubic Hermite polynomials for the two-dimensional solution of the two-group diffusion problem. Two modifications are introduced with respect to the conventional expression for the weak form of the group diffusion equation with the zero flux or zero current boundary condition and the cubic element functions over the boundary nodes. The finite element formulations obtained from those modifications are tested with the two-dimensional ZION problem. The numerical effectiveness of the modifications are examined.

요 약

중성자 다군 확산 방정식의 해를 구하기 위하여 albedo형 경계조건을 Hermite 3차 다항식에 의거한 유한요소법과 결합하였다. 중성자 확산문제에 흔히 이용되는 확산방정식의 weak form을 경계조건과 일치하도록 수정하였으며 또한 경계면에 접한 node영역에서의 요소함수 또한 수정 정의하였다. 수정된 유한요소법의 수치계산상의 효율성을 조사할 목적으로 2차원 ZION 가압경수형 원자로문제를 시험계산하고 그 결과를 기존의 다른 계산결과와 비교하였다.

I. Introduction

Kalambokas and Henry proposed an albedo-type boundary condition[1,2] applicable along the core-reflector interfaces for the solution of the two-group diffusion equation. Their boundary condition enables one to reduce the number of unknowns in discretizing the group diffusion equation by excluding the reflector region from the explicit computational mesh grid, which in turn reduces the computer storage as well as the computer time required for solving the group diffusion equation. They demonstrated[2] that the use of the albedo-type boundary condition could save the computer memory and computing time in two-group diffusion computation of the 2-D ZION reactor with the finite difference diffusion

theory code, CITATION. They further suggested using their boundary condition in the coarse mesh methods like finite element and nodal methods.

Motivated by the suggestion, we attempt herein to incorporate the albedo-type boundary condition into the finite element formulation of the cubic Hermite polynomials[3,4] for the two-dimensional solution of the two-group diffusion problem. In doing so we introduce two modifications. First, the weak form of the group diffusion equation which usually applies to the group diffusion problem with the boundary condition of the zero flux or the zero current is modified to conform itself to the albedo-type boundary condition. Second, the element functions of the cubic Hermite polynomials as specified in refs. 3 and 4 are also modified over the boundary nodes, e.g., the nodes which are in direct contact with the core-reflector interface.

The finite element formulation obtained from these modifications is applied to the two-dimensional ZION PWR problem. The computational effectiveness of the modification is then examined and discussed with regard to the reference results of subassembly power distribution and the effective multiplication of the ZION reactor.

II. Formulation

The problem to be solved is the two-group diffusion equation,

$$-\nabla\cdot[D]\nabla[\phi]+[\Sigma_r][\phi]-\frac{1}{\lambda}[\chi\nu\Sigma_f][\phi]=0 \tag{1}$$

with the albedo-type boundary condition,

$$[\phi(r_s)]=[\alpha][J_n(r_s)], \tag{2}$$

where

$$[D]=\begin{bmatrix} D_1 & 0 \\ 0 & D_2 \end{bmatrix},$$

$$[\Sigma_r]=\begin{bmatrix} \Sigma_1 & 0 \\ -\Sigma_{1\to 2} & \Sigma_2 \end{bmatrix},$$

$$[\chi\nu\Sigma_f]=\begin{bmatrix} \chi_1\nu\Sigma_{f_1} & \chi_1\nu\Sigma_{f_2} \\ \chi_2\nu\Sigma_{f_1} & \chi_2\nu\Sigma_{f_2} \end{bmatrix},$$

and

$$[\alpha]=\begin{bmatrix} \alpha_{11} & 0 \\ \alpha_{21} & \alpha_{22} \end{bmatrix}.$$

The notation in the above is conventional. The $\alpha_{gg'}$ are the albedo constants[1] which relate the normal outward group current J_{gn} to the group fluxes at the core-reflector interface r_s. The finite element solution to Eq.(1) starts with the trial expansion of the group fluxes by the piecewise continuous element functions, $U_{gJ}(r)$, which are suitably defined over the spatial mesh grids of the problem domain,

$$\phi_g(r)=\sum_J \phi_{gJ}U_{gJ}(r) \tag{4}$$

The expansion coefficients ϕ_{gJ} are then determined using the variational principle (see Appendix A),

$$\int_v (\nabla[\delta\phi^*(r)]\ [D]\nabla[\phi]+[\delta\phi^*]([\Sigma_r] -\frac{1}{\lambda}[\chi\nu\Sigma_f])\ [\phi]dv +\sum_s\int_s [\delta\phi^*(r_s)][\beta_s][\phi(r_s)]ds=0, \tag{5}$$

for the arbitrary variation $[\delta\phi^*]$, with $[\beta_s]=[\alpha(r_s)]^{-1}$. Putting

$$\delta\phi_g^*(r)=\sum_J \delta\phi_{gJ}^* U_{gJ}(r) \tag{6}$$

and noting that $\delta\phi_{gJ}^*$ are components of the completely arbitrary vector $[\delta\phi^*]$, we obtain a system of algebraic equations for $[\phi]$=column vector $[\phi_{gJ}]$,

$$[A][\phi]=\frac{1}{\lambda}[M][\phi], \tag{7}$$

where

$$[A]_{gJg'J'}=\delta_{gg'}\int_v \nabla U_{gJ}\ D_{g'}\ \nabla U_{g'J'}dv +\int_v U_{gJ}(\Sigma_g\delta_{gg'}-\Sigma_{gg'})U_{g'J'}dv +\sum_s\int_s U_{gJ}(r_s)\beta_{gg'}U_{g'J'}(r_s)ds$$

$$[M]_{gJg'J'}=\chi_g\int_v U_{gJ}(r)\nu\Sigma_{fg'}U_{g'J'}(r)dv$$

where $\delta_{gg'}$ is the Kronecker delta function and $\Sigma_{gg'}$ the macroscopic scattering cross section

from group g' to group g. Equation (5) is the variational expression for the weak form of the group diffusion equation. It is noted that Eq. (5) differs from the conventional weak form of the group diffusion equation with the zero-flux or zero-current boundary condition in that it contains an additional term arising from the boundary condition of the form, Eq. (2).

The weak form of the group diffusion equation, Eq. (5), is based upon an tacit assumption that the trial solution satisfies the condition of the flux and current continuity across all the internal interfaces. Therefore, the element functions must be chosen to satisfy the condition of the flux and current continuity at least across the internal interfaces. In conjunction with this requirement, we make use of the cubic element functions constructed from the piecewise Hermite interpolation[3,4] as the basis functions for the flux expansion over all the core-interior nodes. As for the element functions over the boundary nodes, we construct them in the following way.

Consider the boundary node, $x\in\{x_{N-1},\ x_N\}$, in the one-dimensional mesh grid shown in Fig. 1. Since the flux and current at $x=x_N$ are interrelated to each other by the boundary condition of Eq. (2), we assume the element function over $x\in\{x_{N-1},\ x_N\}$ is of the form,

$$U_{gN}(x)=\begin{cases} U_N^{0-}(x)+\gamma_{gN}\,U_N^{1-}(x) & x\in\{x_{N-1},\ x_N\} \\ 0 & \text{otherwise} \end{cases} \tag{8}$$

where U_N^{0-} and U_N^{1-} are the piecewise cubic Hermite polynomials.

Requiring that the trial expansion for the 1-D group flux,

$$\phi_g(x)=\sum_{i=1}^{N-1}\{\phi_{gi}U_{gi}^0(x)+J_{gi}U_{gi}^1(x)\}$$

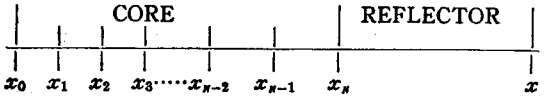

Fig. 1. One-Dimensional Mesh Grid

$$+\phi_{gN}U_{gN}(x),$$

satisfy the boundary condition, Eq.(2), we find the γ_{gN} is given by

$$\gamma_{gN}=-\beta_{gg}+\beta_{12}\delta_{g2}C_N;\ C_N=\phi_{1N}/\phi_{2N} \tag{9}$$

The 1-D element function $U_{gN}(x)$ can be used for constructing the two- and three-dimensional element functions over the boundary nodes. With the 2-D application in mind,we note that three types of the boundary nodes are identified according to the way the boundary nodes contact with the reflector, as shown in Fig. 2. The 2-D element functions associated with the boundary nodes of Fig. 2(a) are

$$U_{gij}^{00}(x,y)=\begin{cases} 0 & x,y\in I \\ U_i^{0-}(x)\ U_j^{0+}(y) & x,y\in II \\ U_i^{0-}(x)\ U_j^{0-}(y) & x,y\in III \\ U_i^{0+}(x)\ U_j^{0-}(y) & x,y\in IV \end{cases} \tag{10}$$

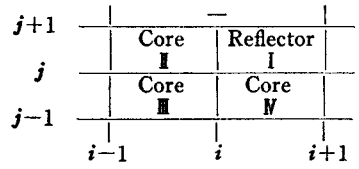

2(a)

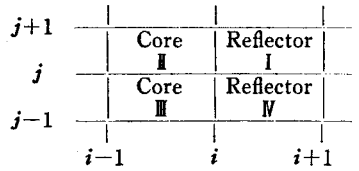

2(b)

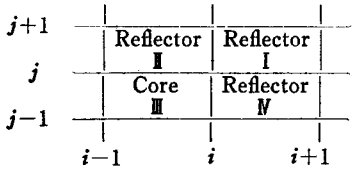

2(c)

Fig. 2. Rectangular Elements at the Boundary Node in Two-Dimensional Space.

$$U^{01}_{gij}(x,\ y)=\begin{cases}\left(U^{0-}_i(x)+\dfrac{\gamma_{gi}}{D_{gII}}\ U^{1-}_i(x)\right)U^{1+}_j(y) & x,y\in II\\ U^{0-}_i(x)\ U^{1-}_j(y) & x,y\in III\\ 0 & \text{otherwise}\end{cases}\tag{11}$$

$$U^{10}_{gij}(x,\ y)=\begin{cases}U^{1-}_i(x)\ U^{0-}_j(y) & x,y\in III\\ U^{1+}_i(x)\left(U^{0-}_j(y)+\dfrac{\gamma_{gj}}{D_{gIV}}\ U^{1-}_j(y)\right) & x,y\in IV\\ 0 & \text{otherwise}\end{cases}\tag{12}$$

The element functions associated with the boundary nodes of Fig. 2(b) are

$$U^{0}_{gij}(x,\ y)=\begin{cases}\left(U^{0-}_i(x)+\dfrac{\gamma_{gi}}{D_{gII}}\ U^{1-}_i(x)\right)U^{0+}_j(y) & x,y\in II\\ \left(U^{0-}_i(x)+\dfrac{\gamma_{gi}}{D_{gIII}}\ U^{1-}_i(x)\right)U^{0-}_j(y) & x,y\in III\\ 0 & \text{otherwise}\end{cases}\tag{13}$$

$$U^{1}_{gij}(x,\ y)=\begin{cases}\left(U^{0-}_i(x)+\dfrac{\gamma_{gi}}{D_{gII}}\ U^{1-}_i(x)\right)\dfrac{\theta}{D_{gII}}\ U^{1+}_g(y) & x,y\in II\\ \left(U^{0-}_i(x)+\dfrac{\gamma_{gi}}{D_{gIII}}\ U^{1-}_i(x)\right)\dfrac{\theta}{D_{gIII}}\ U^{1-}_j(y) & x,y\in III\\ 0 & \text{otherwise}\end{cases}$$

Finally, the element function associated with the boundary nodes of Fig. 2(c) is

$$U_{gij}(x,\ y)=\begin{cases}\left(U^{0-}_i(x)+\dfrac{\gamma_{gi}}{D_{gIII}}\ U^{1-}_i(x)\right)\left(U^{0-}_j(y)+\dfrac{\gamma_{gi}}{D_{gIII}}\ U^{1-}_j(y)\right) & x,y\in III\\ 0 & \text{otherwise}\end{cases}$$

The 2-D element functions in Eqs. (10)~(15) are constructed such that the trial flux expansion, Eq. (4), satisfy the boundary condition. A special feature of these element functions is that they depend on the expansion coefficient ϕ_{gN} which is priori unknown. In this sense they may be called the implicit type. On the other hand, the variational principle, Eq. (5), accepts the arbitrary flux expansion as the trial solution of the group diffusion equation so far as it satisfies the condition of the continuity across all the internal interfaces. It doesn't matter whether or not the trial solution satisfies the boundary condition. This fact allows us to construct the element functions over the boundary nodes in the explicit way. We construct the explicit type of the element functions simply by putting $\gamma_{gN}=-\beta_{gg}(r_N)$.

III. Numerical Results and Discussions

The finite element formulation as described above is applied for the computations of the two-dimensional gross power distribution and the effective multiplication in the ZION reactor. The ZION reactor is a checkerboard-loaded PWR, and representative of the medium-sized reactor of its kind. Fig. 3 depicts the geometrical arrangements of the reactor components. Table 1 lists the two-group cross sections of the material composition.

The finite element computation for the 2-D power of the ZION reactor is performed with two types of the boundary-node element functions; the implicit type and the explicit type. As for the parameters, $\alpha_{gg'}$, the composite slab albedo values[1,2] are utilized to represent the bou-

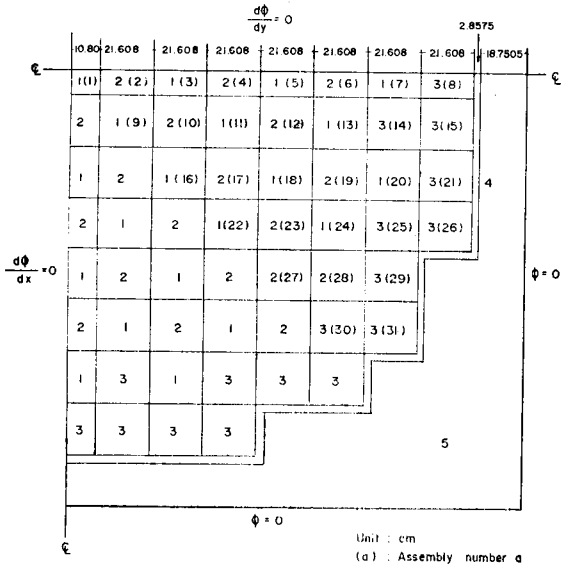

Fig. 3. Geometry of the Two-Dimensional ZION First Core

ndary condition along the core-reflector interfaces except the 90-degree wedge shaped interfaces. The enumeration of the $\alpha_{gg'}$ for the wedged portion of interfaces requires a complicated numerical integration.[1,2] In this application, however, an empirical factor 1.3 is applied to the composite slab albedo values to account for the neutron reentrance effects.

Figure 4 shows the results of the present finite element computations for the normalized subassembly power distribution of the ZION reactor. Table 2 compares the normalized subassembly power of the finite element computations with various other calculations. These results indicate that the finite element computations compare fairly well with the results of other methods. With the CITATION 75×75 computation taken as the reference, the 1-node-per-fuel-assembly finite element computation with the implicit type of element functions results in the core-mean relative errors of 1.02% in the subassembly power ratios while the same computation with the explicit type of element functions gives rise to the corresponding error of 0.85%. The computation with the reduced mesh width, e.g., 2×2 nodes per fuel assembly,

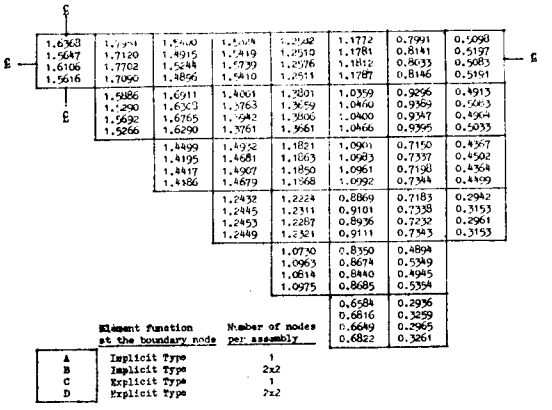

Fig. 4. Normalized Subassembly Power Distribution of the ZION PWR

Table 1. Macroscopic Cross Sections for the Two-Dimensional ZION Problem

Region	Group	D(cm)	Σ_a(cm^{-1})	$\nu\Sigma_f$(cm^{-1})	$\Sigma_{1\to2}$ (cm^{-1})
1 (2.25% enriched fuel)	1	1.41760	0.02597	0.00536	0.01742
	2	0.37335	0.06669	0.10433	—
2 (2.8% enriched fuel)	1	1.41970	0.02576	0.00601	0.01694
	2	0.37370	0.07606	0.12472	—
3 (3.3% enriched fuel)	1	1.42650	0.02560	0.00653	0.01658
	2	0.37424	0.08359	0.14120	—
4 (baffle)	1	1.02130	0.00322	0.0	0.0
	2	0.33548	0.14596	0.0	—
5 (reflector)	1	1.45540	0.02950	0.0	0.02903
	2	0.28994	0.00949	0.0	—

Table 2. Comparison of Finite Element Computation for the Normalized Assembly Powers With Other Computations

Method	CITATION*	PDQ-5*	CHD*	Present Computation			
				Implicit Type		Explicit Type	
No. of unknowns per group	5625 (75×75)	1936 (44×44)	348 (10×10)	227 ($9^{-}\times9^{-}$)	775 ($16^{-}\times16^{-}$)	227 ($9^{-}\times9^{-}$)	775 ($16^{-}\times16^{-}$)
Assembly Number	Average Assembly Power						
1	1.6271	1.6361	1.6524	1.6368	1.5647	1.6106	1.5616
2	1.7590	1.8002	1.8108	1.7951	1.7120	1.7702	1.7090
3	1.5320	1.5387	1.5524	1.5400	1.4915	1.5244	1.4896
4	1.5519	1.5856	1.5918	1.5824	1.5419	1.5739	1.5410
5	1.2537	1.2560	1.2623	1.2582	1.2510	1.2576	1.2511
6	1.1587	1.1758	1.1742	1.1772	1.1781	1.1812	1.1787
7	0.8039	0.7904	0.7896	0.7991	0.8141	0.8033	0.8146
8	0.5115	0.4954	0.4871	0.5098	0.5197	0.5083	0.5191
9	1.5800	1.5873	1.6025	1.5886	1.5290	1.5692	1.5266
10	1.6563	1.7051	1.7038	1.6911	1.6308	1.6765	1.6290
11	1.3945	1.3990	1.4087	1.4001	1.3768	1.3942	1.3761
12	1.3556	1.3818	1.3841	1.3801	1.3659	1.3806	1.3661
13	1.0372	1.0318	1.0339	1.0359	1.0460	1.0400	1.0466
14	0.9166	0.9230	0.9186	0.9296	0.9389	0.9347	0.9395
15	0.4790	0.4786	0.4705	0.4913	0.5038	0.4904	0.5033
16	1.4452	1.4490	1.4603	1.4499	1.4195	1.4417	1.4186
17	1.4664	1.4966	1.5023	1.4932	1.4681	1.4907	1.4679
18	1.1831	1.1813	1.1859	1.1821	1.1863	1.1850	1.1868
19	1.0779	1.0903	1.0878	1.0901	1.0983	1.0961	1.0992
20	0.7262	0.7092	0.7078	0.7150	0.7337	0.7198	0.7344
21	0.4455	0.4285	0.4206	0.4367	0.4502	0.4364	0.4499
22	1.2447	1.2439	1.2493	1.2432	1.2445	1.2453	1.2449
23	1.2123	1.2255	1.2257	1.2224	1.2311	1.2287	1.2321
24	0.9001	0.8872	0.8869	0.8869	0.9101	0.8936	0.9111
25	0.7216	0.7123	0.7067	0.7183	0.7338	0.7232	0.7343
26	0.3233	0.3013	0.2911	0.2942	0.3153	0.2961	0.3153
27	1.0777	1.0749	1.0747	1.0730	1.0963	1.0814	1.0975
28	0.8526	0.8401	0.8379	0.8350	0.8674	0.8440	0.8685
29	0.5340	0.5104	0.5019	0.4894	0.5349	0.4945	0.5354
30	0.6682	0.6516	0.6462	0.6584	0.6816	0.6649	0.6822
31	0.3277	0.3042	0.2947	0.2936	0.3259	0.2965	0.3261

* data from ref. 4

reduces these errors further to the order of 0.4%. As for the k_{eff}, the present computations predict it with the mean relative deviation of less than 0.05% regardless of the mesh width and the type of element functions.

The computational accuracy did not show any dependency on the type of the element functions adopted for the boundary nodes. From the standpoint of the computational time, however, the explicit type of element functions have the slight advantage over the implicit type of element functions. This is because the latter contains the C_N, the fast to thermal flux ratio at the nodal points along the core-reflector interface and

Table 3. Summary of the Results for the Two-Dimensional ZION Problem

Method	CITATION*	PDQ-5*	CHD*	Present Computation			
				Implicit Type		Explicit Type	
No. of unknowns per group	5625 (75×75)	1936 (44×44)	348 (10×10)	227 ($9^{-}\times9^{-}$)	775 ($16^{-}\times16^{-}$)	227 ($9^{-}\times9^{-}$)	775 ($16^{-}\times16^{-}$)
Effective multiplication factor k_{eff}	1.27508	1.2749	1.27469	1.27486	1.27452	1.27456	1.27449
% deviation in k_{eff}	—	0.014	0.031	0.017	0.044	0.041	0.046
Maximum relative errors in power density (%)	—	7.171	10.07	10.41	3.835	9.521	4.026
Core-mean relative error in power density (%)	—	0.906	1.375	1.018	0.342	0.832	0.358
Convergence criteria	4×10^{-4}	4×10^{-4}	1.7×10^{-4}	10^{-4}	4×10^{-4}	10^{-4}	4×10^{-4}
Number of iterations	—	—	—	124	111	89	109
Computing time (sec)	—	—	—	298	926	200	907
Computer system	—	—	—	CDC6400	CDC6400	CDC6400	CDC6400

* data from ref. 4

this ratio must be updated repeatedly during the course of the outer iteration. The difference of the computing time shown in the 7th row of Table 3 is due to the additional computation required for updating the C_N's in using the explicit type of element functions.

IV. Conclusion

The major advantage of the finite element formulation presented in this paper stems from the fact that it involves the relatively fewer number of the unknowns in comparison with the usual formulation which includes the reflector region into the explicit computational mesh. Since it involves the fewer unknowns, the lower computer memory and the less computing time is required for the gross power computations. In the case of the ZION reactor, it is observed that the present formulation saves the computer storage requirements by roughly one-fourth and the computing time by more than 10%. In view of this saving as well as the good computational accuracy, the present finite element formulation remains promising as an efficient computational method for the multi-dimensional power computation.

References

1) P.C. Kalambokas and A.F. Henry, "The Replacement of Reflectors by Albedo Type Boundary Conditions," Proc. Conf. on Computational Method in Nuclear Engineering, CONF-750413, **I**, I-25, ANS (1975)
2) P.C. Kalambokas and A.F. Henry, *Nucl. Sci. Eng.* **61**, 181 (1976)
3) C.M. Kang and K.F. Hansen, *Nucl. Sci. Eng.* **51**, 456 (1973)
4) L.O. Deppe and K.F. Hansen, *Nucl. Sci. Eng.* **54** (1974)

Appendix A. Variational Expression for the Weak Form of Group Diffusion Equation

Consider a functional $F_d([\phi], [\phi^*])$

$$F_d = \frac{\int_v dv\{[\phi^*]^T[\Sigma_r][\phi]+\nabla[\phi^*][D]\nabla[\phi]\}}{\int_v[\phi^*]^T[\chi\nu\Sigma_f][\phi]dv} + \frac{\sum_s\int_s ds[\phi^*(r_s)][\beta_s][\phi(r_s)]}{\int_v[\phi^*]^T[\chi\nu\Sigma_f]\ [\phi]\ dv.} \tag{A-1}$$

Taking an arbitrary variations in argument functions of F_d, we can show that the lst order variation δF_d is given by

$$\begin{aligned}\delta F_d &= F_d([\phi+\delta\phi], [\phi^*+\delta\phi^*]) - F_d([\phi], [\phi^*])\\ &= \left\{\int_v [\phi^*]^T[\chi\nu\Sigma_f][\phi]dv\right\}^{-1}\\ &\quad \left\{\int_v [\delta\phi^*]^T\left\{-\nabla\cdot[D]\nabla+[A]-\frac{1}{\lambda}[\chi\nu\Sigma_f]\right\}[\phi]dv\right.\\ &\quad +\sum_s\int_s [\delta\phi^*(r_s)]^T\{[D]\nabla[\phi(r_s)]\cdot\boldsymbol{n}+\\ &\quad [\beta_s][\phi(r_s)]\}ds\\ &\quad +\int_v [\delta\phi]^T\left\{-\nabla\cdot[D]\nabla+[A]-\frac{1}{\lambda}[\chi\nu\Sigma_f]^T\right\}[\phi^*]dv\\ &\quad +\sum_s\int_s [\delta\phi]^T\{[D]\nabla[\phi^*(r_s)]\cdot\boldsymbol{n}+[\beta_s]^T[\phi(r_s)]\}ds\\ &\quad \left.+0(\delta^2)\right\}.\end{aligned}$$

$0(\delta^2)$ denotes the second order term in the arbitrary variation in $\delta\phi_g$ or $\delta\phi_g^*$. The stationary value of F_d is denoted by λ.

From Eq. (A-2), it is clearly seen the condition that the first order variation δF_d vanishes for a completely arbitrary variation in $[\phi]$ and $[\phi^*]$ leads to the original group diffusion problem with the albedo-type boundary condition and the adjoint problem alike. Finally, noting

$$[\delta\phi^*]^T\nabla\cdot[D]\nabla[\phi] = \nabla\cdot[\delta\phi^*]^T[D]\nabla[\phi] - \nabla[\delta\phi^*]^T[D]\nabla[\phi]$$

and

$$\int_v \nabla\cdot[\delta\phi^*]^T[D]\nabla[\phi]\ dv = \sum_s\int_s \nabla[\delta\phi^*]^T[D]\nabla[\phi]\cdot\boldsymbol{n}ds,$$

we find

$$\begin{aligned}\delta F_d = 0 = &\int_v \{[\delta\phi^*]^T([A]-\frac{1}{\lambda}[\chi\nu\Sigma_f])\ [\phi]\\ &+\nabla[\delta\phi^*]^T[D]\nabla[\phi]\}\ dv\\ &+\sum_s\int_s [\delta\phi^*(r_s)]^T[\beta_s][\phi(r_s)]\ ds\\ &+\int_v \{[\delta\phi]^T([A]-\frac{1}{\lambda}[\chi\nu\Sigma_f]^T)\ [\phi^*]\\ &+\nabla[\delta\phi]^T[D]\nabla[\phi^*]\}dv\\ &+\sum_s\int_s [\delta\phi(r_s)]^T[\beta_s]^T[\phi^*(r_s)]ds.\end{aligned} \tag{A-3}$$

Eq. (A-3) is the weak form of the group diffusion equation equivalent to the original group diffusion problem with the boundary condition specified by Eq. (2).